

The evaluation of the role of C–H···F hydrogen bonds in crystal altering the packing modes in the presence of strong hydrogen bond

Gurpreet Kaur ¹, Sandhya Singh ¹, Amritra Sreekumar, Angshuman Roy Choudhury *

Department of Chemical Sciences, Indian Institute of Science Education and Research (IISER) Mohali, Sector 81, Knowledge City, S. A. S. Nagar, Manauli PO, Mohali, 140306, Punjab, India

ARTICLE INFO

Article history:

Received 13 August 2015

Received in revised form

29 October 2015

Accepted 30 October 2015

Available online 6 November 2015

Keywords:

N-benzylideneanilines

C–H···F hydrogen bond

Gaussian09

AIM2000

Weak interactions

Organic fluorine

Benzylideneanilines

CLP

ABSTRACT

Interactions involving fluorine is an area of contemporary research. To unravel the importance of weak C–H···F hydrogen bonds and C–H···π interactions in organic compounds in the presence of strong hydrogen bond, a series of *N*-benzylideneanilines with simultaneously hydroxyl (–OH) and fluorine substitutions were synthesized for structural analysis. These compounds have been studied through experimental single crystal X-ray diffraction analysis and computational methods (Gaussian09 and AIM2000). The hydroxyl group present in all the molecules were found to form strong O–H···N hydrogen bond, but the spatial arrangement of the molecules connected by this hydrogen bond have been found to be controlled by the weak C–H···F and C–H···O hydrogen bonds, weak C–H···π and π···π interactions. This manuscript illustrates the importance of several weaker interactions in altering the packing modes in the presence of strong hydrogen bonds.

© 2015 Elsevier B.V. All rights reserved.

1. Introduction

Crystal engineering deals with the understanding of both strong and weak intermolecular forces to build a desired three dimensional architecture to achieve robust molecular framework for advanced applications [1]. A clear understanding of strong and weak interactions is needed for appropriate applications of crystal engineering to design different functional materials. Crystallization of molecules from different solvents and solvent mixtures or by using different crystallization techniques are known to result into different crystal structures (polymorphs) of the same compound [2]. The connection between molecular structure and its crystal structure can only be achieved through an understanding of intermolecular interactions in the solid state [3]. Various strong and weak intermolecular forces include strong and weak hydrogen bonds [3], interaction involving halogens [4], X–H···π (X = C, N, O) interactions [5], π···π interactions [6] etc. The molecules, which pack in the crystal lattice through strong hydrogen bonds are

known to yield highly stable crystal structures thereby making it difficult to alter the packing features through small alteration in the parent molecule [7]. On the other hand, the crystal structures governed by only weak hydrogen bonds or by a combination of strong and a number of weak hydrogen bonds are altered easily by minor changes in the parent molecule [8]. Weaker hydrogen bonds result into lower stabilization energies while forming molecular assemblies by the formation of dimers, trimers, tetramers, chains, ladders, ribbons etc. [9] Therefore, crystal structures governed by these interactions can easily be altered by the incorporation of other functional groups. Among the weak hydrogen bonds, the interactions offered by “organic fluorine” [10] are of specific interest because of its ambiguous behaviour [11] in the solid state. In spite of the highest electronegativity of fluorine, it was considered to be weaker electron acceptor than oxygen or nitrogen and was refuted to have true hydrogen bonds by Howard et al. [11c] Thalladi et al. [12] for the first time glorified the role of C–H···F interactions in their structural investigations on fluoro-benzenes using newly developed techniques of in-situ crystallization [12,13]. In the last decade, a number of research groups have illustrated that organic fluorine offers various intermolecular interactions such as C–H···F–C, C–F···X–C (X = F, Cl, Br) and C–F···π [14]. The significance of these interactions in crystal engineering have been

* Corresponding author.

E-mail address: angshurc@iisermohali.ac.in (A.R. Choudhury).

¹ These two authors have contributed equally towards this manuscript.

highlighted in the review by Berger et al. [15], by Chopra and Guru Row [16] in their recent highlight and further by Chopra in his perspective [17]. The polarizability of organic fluorine was earlier refuted based on the high electronegativity of F. A recent experimental charge density study first revealed the formation of sigma hole on fluorine thereby indicating that organic fluorine is also partially polarizable [18].

Since, the interactions offered by organic fluorine are generally weak in nature, their application in crystal engineering has mostly been studied in the absence of any strong hydrogen bond donor and acceptors group(s) [9a-d,14a-d]. Our recent structural investigations in a series of *N*-benzylideneaniline and azobenzene indicate that the weak interactions offered by organic fluorine are capable of offering various repetitive supramolecular synthons through C–H···F–C hydrogen bonds [9a-d]. In this manuscript, we intend to evaluate the structure directing/controlling ability of organic fluorine in the presence of a hydroxyl group in fluorinated *N*-benzylideneanilines. These molecules containing simultaneously –OH and C–F groups offer an opportunity for a systematic analysis of weak hydrogen bonds offered by the C–F group in the presence of strong hydrogen bonds involving the –OH group. We have structurally analysed and computationally studied these molecules to achieve an understanding of the individual roles played by organic fluorine and the hydroxyl group in crystal packing. Our earlier structural studies on *N*-benzylideneanilines contained structures of 87 compounds (1 to 87) [9a,c,d]. Therefore, the new compounds studied in this manuscript have been numbered from 88 to 111 so that direct comparison can be made with the previously reported structures.

2. Experimental section

2.1. Procedure for synthesis

All the starting materials were purchased from Sigma Aldrich and were used without further purification. All the compounds were synthesized using the mechano-chemical approach [19]. Corresponding benzaldehyde (0.5 mmol) and aniline (0.5 mmol) were ground using mortar and pestle with approximately 100 µl methanol. The resulting mixture slowly solidified upon grinding for 10–15 min to yield the desired product. The solid crude products were then dissolved in various solvents (methanol, ethanol, hexane, ethyl acetate, chloroform and dichloromethane) and the solutions were allowed to evaporate slowly in refrigerator (4 °C) for recrystallization and subsequent growth of single crystals suitable for structure determination.

Scheme 1 describes all the molecules studied and the method of nomenclature used in this manuscript. Based on the nature and position of the substitutions, the compounds have been sub divided into 6 groups as indicated in the **Scheme 1**. Out of 24 synthesized compounds, 20 compounds yielded single crystals of good quality for structural analysis. Remaining four compounds (C.N. 100, 101, 102 and 103), although crystalline (PXRD pattern in ESI), have always resulted into the glassy material during the recrystallization process.

All the synthesized compounds were characterized by ¹H NMR (400 MHz, Bruker Biospin Advance-III NMR spectrometer) (ESI, Fig. S2: 1 to 20) and FTIR (Perkin Elmer Spectrum2) (ESI, Fig. S3: 1 to 20) spectroscopy. Powder X-ray Diffraction (PXRD) data were recorded on a Rigaku Ultima IV diffractometer using parallel beam geometry, Cu – K α radiation, 2.5° primary and secondary solar slits, 0.5° divergence slit with 10 mm height limit slit, sample rotation stage (120 rpm) attachment and DTex

Ultra detector at 40 kV of tube voltage and 40 mA of the current. The data sets were collected over 20 ranging from 5 to 50° with a scanning speed of 5° per minute with 0.02° step for all the compounds.

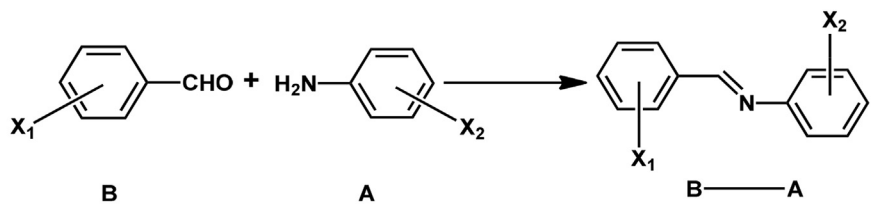
The PXRD patterns have been simulated from the crystal coordinates using Mercury [20] and compared with the observed PXRD patterns using WINPLOTR²¹⁰ (ESI, Fig. S4: 1 to 24). The simulated PXRD patterns were found to match with the experimentally observed PXRD recorded on the bulk sample. This indicates that the bulk phase is represented by the structure determined by the single crystal X-ray diffraction technique. Melting points and the melting enthalpies of all the compounds (Table S1) were determined from the DSC (Perkin Elmer DSC 8000) traces recorded at 5° per minute heating rate under Nitrogen atmosphere (ESI, Fig. S5: 1 to 24).

3. Diffraction data collection and structure solution

Single crystal X-ray diffraction data for the crystals were recorded using Mo – K α radiation at 100.0(1) K using Oxford cryosystem either on Bruker AXS KAPPA APEX-II CCD diffractometer or on a Rigaku XtalAB mini diffractometer using Mercury375/M CCD detector using graphite monochromator. The data sets, which collected on Bruker diffractometer were recorded using a detector distance of 6.0 cm with varying 2θ position of the detector using the APEX-II suit [22], data reduction and integration were performed SAINT V7.685A12 [22] (Bruker AXS, 2009) and absorption corrections and scaling were done using SADABS V2008/112 [22] (Bruker AXS). The remaining data sets collected on XtalAB mini diffractometer were recorded using a fixed detector distance of 5.0 cm and the detector kept at 2θ = 29.85° and were processed with Rigaku Crystal Clear suite 2.0 [23]. All the crystal structures were solved using SHELXS [24] and were refined using the SHELXL [24] available within Olex2 [25]. All the hydrogen atoms have been geometrically fixed and refined using the riding model except the hydrogen of the –OH group, which has been located from the difference Fourier map and was refined isotropically. Complete crystal data collection and refinement details for all the compounds are available in the Tables S1a–d (ESI). The thermal ellipsoid plots of all the molecules have been drawn at 50% probability for the non-H atoms using Mercury and are shown with the atom labels in the ESI (Fig. S6: 1 to 20). All the packing and interaction diagrams have been generated using Mercury 3.5 [20]. Geometric calculations have been done using PARST [26] and PLATON [27].

3.1. Crystallographic modelling of disorder

Among the 20 compounds reported in this manuscript, the compound 90 was found to have positional disorder due to rotation of the aniline ring around C8–N1 bond and the compounds 104 and 108 were found to exhibit positional disorder due to in-plane flipping of the molecule around C=N bond. PART command was used to analyse these positional disorders. These disorders were refined for two independent positions, namely A and B ('A' for higher occupancy). For the purpose of refinement, the position of the carbon atoms in part A and B of the phenyl rings were fixed at the same position using EXYZ command in SHELXL2013. Thermal parameters were also constrained to be equal for the atoms at the same position using EADP command in SHELXL2013. All hydrogen atoms were then positioned geometrically and refined using a riding model with U_{iso} (H) = 1.2 U_{eq} (C, N). The occupancy ratio for the two parts in 90, 104 and 108 were



Where $X_1, X_2 = -F, -H, -OH; X_1 \neq X_2$

Group 1a			Group 1b		
No.	X_1	X_2	No.	X_1	X_2
88	<i>p</i> -OH	H	92	H	<i>p</i> -OH
89	<i>p</i> -OH	<i>p</i> -F	93	<i>p</i> -F	<i>p</i> -OH
90	<i>p</i> -OH	<i>m</i> -F	94	<i>m</i> -F	<i>p</i> -OH
91	<i>p</i> -OH	<i>o</i> -F	95	<i>o</i> -F	<i>p</i> -OH
Group 2a			Group 2b		
No.	X_1	X_2	No.	X_1	X_2
96	<i>m</i> -OH	H	100*	H	<i>m</i> -OH
97	<i>m</i> -OH	<i>p</i> -F	101*	<i>p</i> -F	<i>m</i> -OH
98	<i>m</i> -OH	<i>m</i> -F	102*	<i>m</i> -F	<i>m</i> -OH
99	<i>m</i> -OH	<i>o</i> -F	103*	<i>o</i> -F	<i>m</i> -OH
Group 3a			Group 3b		
No.	X_1	X_2	No.	X_1	X_2
104	<i>o</i> -OH	H	108	H	<i>o</i> -OH
105	<i>o</i> -OH	<i>p</i> -F	109	<i>p</i> -F	<i>o</i> -OH
106	<i>o</i> -OH	<i>m</i> -F	110	<i>m</i> -F	<i>o</i> -OH
107	<i>o</i> -OH	<i>o</i> -F	111	<i>o</i> -F	<i>o</i> -OH

(*) indicates the compounds which did not give good quality single crystals.

Scheme 1. Numbering scheme and systematic identification numbers of the compounds studied.

found to be 0.882(3): 0.118(3), 0.506(7): 0.494(7) and 0.896(3): 0.104(3) respectively.

4. Theoretical calculations

4.1. Stabilization energy calculations by Gaussian09

The crystal structures reported in this manuscript are found to be controlled by combined effects of strong ($O-H\cdots N$) and weak ($C-H\cdots O$, $C-H\cdots F$) hydrogen bonds and much weaker interactions involving the aromatic π systems ($C-H\cdots\pi$ and $\pi\cdots\pi$). As we are interested to evaluate the ability of organic fluorine in altering the crystal packing in the presence of other stronger hydrogen bonds,

the stabilization energies of the molecular dimers formed through $O-H\cdots N$ or $C-H\cdots O$ or $C-H\cdots F$ hydrogen bonds have been calculated using the MP2 [28] level of theory with 6-31 + G(d) basis set using the Gaussian09 [29] as has been described in detail in our earlier publication [9c]. The pairs of molecules, which are found to be connected with each other by $O-H\cdots N/C-H\cdots O/C-H\cdots F$ hydrogen bonds, were selected for the calculation of single point energy of the dimer (E_{dimer}) and the single point energy of the corresponding monomers were also calculated using Gaussian09 in the same method and same basis set. The stabilization energies ($SE_{\text{G09}} = E_{\text{dimer}} - 2 \times E_{\text{monomer}}$) of these dimers were corrected for the basis set superposition error (BSSE) using the counterpoise method [30]. GaussView [31] was used to visualize the molecular

dimers while the Gaussian calculation were carried out.

4.2. Coulomb–London–Pauli (CLP) energy calculations

The lattice energies of these crystal structures were calculated using the semi-classical density sums (SCDS) PIXEL method [32], which was implemented within the 2011 version of the CLP model of intermolecular interaction package. This calculation further partitioned the lattice energy into columbic (E_{COUL}), polarization (E_{POL}), dispersion (E_{DISP}) and repulsion (E_{REP}) components.

4.3. Analysis of topological properties

The wave function files for the interacting dimers were generated using the Gaussian09. These wave function files were then used as inputs for AIM2000 package [33] for the analysis of topological parameters like electron densities (ρ_c) and Laplacian ($\nabla^2 \rho_c$) at the bond critical points (BCP). These topological properties provide the information about the nature of the concerned interaction. The topological properties like electron density (ρ) and Laplacian ($\nabla^2 \rho$), local potential ($V(\mathbf{r}_{\text{CP}})$), kinetic ($G(\mathbf{r}_{\text{CP}})$) and total energy densities ($E(\mathbf{r}_{\text{CP}})$) at the BCPs of C–H···F hydrogen bonds have been plotted against bond path (R_{ij}) using sigma plot [34].

5. Structural description of the compounds studied

Here, we intend to discuss the effect of the position of fluorine on the crystal structures of our model system by keeping the position of the –OH substitution constant in one ring, while the position of the fluorine atom is varied on the other ring. Following this method, 24 compounds have been subdivided into six classes namely group 1a, group 1b, group 2a, group 2b, group 3a and group 3b (Scheme 1). The phenyl ring originating from aniline is designated as the “A” ring, while the same originating from the benzaldehyde will be designated as the “B” ring.

5.1. Structural comparison of the compounds belonging to group 1a

Among the compounds belonging to this group (**88**, **89**, **90** and **91**), **88** and **90** are iso-structural (*Pbca*), while **89** and **91** are different from the other two (space groups *Pca2*₁ and *P2/c* respectively) (Table 1). All the four compounds have been found to form dimers involving O–H···N and C–H···O hydrogen bonds together forming a seven membered ring (Fig. 1), which can be designated with the graph set notation $R_2^2(7)$ as described by Etter [35]. These dimers have been found to have stabilization energies between –6.4 and –9.3 kcal/mol (Table 2).

The compounds **89**, **90** and **91** contain fluorine at *para*-, *meta*- and *ortho*-position of the A ring respectively. In case of **89**, the C–H···F hydrogen bond involving F1 and H13 connects two $R_2^2(7)$ dimers formed by O–H···N and C–H···O hydrogen bonds (Fig. 2a). In the case of **90**, a pair of C–H···F hydrogen bonds involving F1 and H11 connects two $R_2^2(7)$ dimers (Fig. 2b) utilizing the synthon II [9d], identified by us recently. A C–H···F hydrogen bond involving F2 and H16 similarly connects two $R_2^2(7)$ dimers (Fig. 2c) in **91**. Although the $R_2^2(7)$ dimers are common in all the structures belonging to this group, the way these dimers are connected to each other in the crystal lattice through weak C–H···F hydrogen bond(s) is different in **89**, **90** and **91**. One of the two molecules present in the asymmetric unit of **91** did not have any interaction involving the fluorine atom.

In addition to the resemblance in the formation of strong hydrogen bonded chains of dimers, similarity in the weak C–H···π interactions (involving H7 with Cg1 and H9 with Cg2) have also been identified in the structures of **88**, **89** and **90** (Fig. 3, Table 3a). In the case of **91**, weak π···π interactions have also been observed between two $R_2^2(7)$ dimers (Fig. 3d, Table 3b).

5.2. Structural comparison of the compounds belonging to group 1b

All the four compounds belonging to this group (**92**, **93**, **94** and **95**) crystallize in the monoclinic centrosymmetric *P2₁/c* space group (Table 4). The compounds **92** and **94** are isostructural, but **93** and **95** adopt different unit cell parameters. All the four compounds have the same $R_2^2(7)$ dimers formed by strong O–H···N and C–H···O hydrogen bonds as were seen in all four compounds belonging to group 1a (Fig. 4, Table 5). The stabilization energies for these dimers are in the range between –7.3 and –12.5 kcal/mol. The dimer in **95** has the highest stabilization energy as it has one O–H···N hydrogen bond and two C–H···O hydrogen bonds forming the dimer (Fig. 4d).

In the structures of **92**, **93**, **94** and **95**, the $R_2^2(7)$ dimers are connected to each other by C–H···F and/or C–H···O hydrogen bonds (Fig. 5, Table 5). Both **92** and **94** have additional C–H···O hydrogen bonds involving H1A with O1 and H9 with O1 (Fig. 5, Table 5). The fluorine atom present at the *meta*-position of the A ring in **94** is involved in a short contact with H6 (Fig. 5, Table 5). Interestingly, the *ortho*-fluorinated compound (**95**) forms a dimer (Fig. 5, Table 5) adopting the robust synthon IV involving two different C–H···F hydrogen bonds reported by us recently [9d].

In addition to these interactions, there are different weak C–H···π interactions in the structure of **92**, **93** and **94** (Table 6). The $R_2^2(7)$ dimers in **92**, **93** and **94** are connected to each other by utilizing two C–H···π interactions between a pair of dimers (Fig. 6a, b

Table 1
Unit cell parameters of the compounds belonging to group 1a (**88**, **89**, **90**, **91**) compounds.

Identification code	88	89	90	91
CCDC No.	1040698	1040699	1040700	1040701
Crystal system	Orthorhombic	Orthorhombic	Orthorhombic	Monoclinic
Space group	<i>Pbca</i>	<i>Pca2</i> ₁	<i>Pbca</i>	<i>P2/c</i>
a/Å	10.8047(6)	10.9585(12)	10.879(2)	19.737(4)
b/Å	9.4127(5)	9.7492(10)	9.323(2)	6.1175(14)
c/Å	19.9210(11)	9.4677(9)	19.888(4)	18.701(4)
α/°	90	90	90	90
β/°	90	90	90	118.201(4)
γ/°	90	90	90	90
Volume/Å ³	2025.99(19)	1011.50(18)	2017.1(8)	1989.9(8)
Z	8	4	8	8
Z'	1	1	1	2

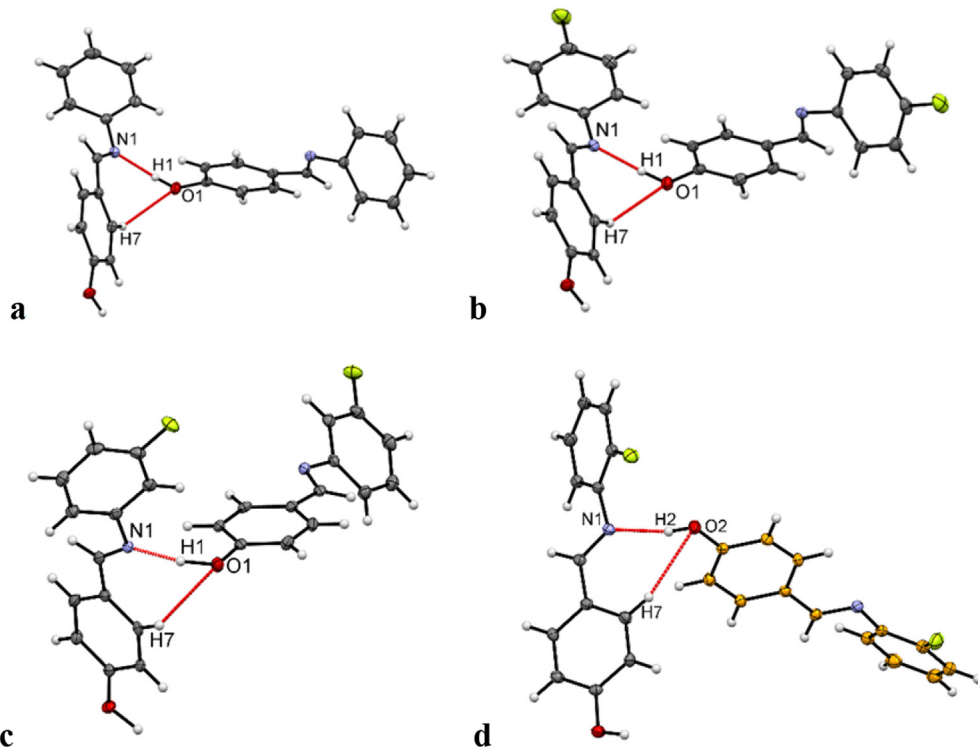


Fig. 1. O–H···N and C–H···O hydrogen bonded dimers in **88** (a), **89** (b), **90** (c) and **91** (d).

Table 2

Intermolecular hydrogen bonds of the compounds belonging to group 1a (**88**, **89**, **90**, **91**) compounds.

Code	D–H···A (D = C, O; A = O, N, F)	d H···A/Å	∠D–H···A/°	Symmetry code	SE _{G09} kcal/mol	ρ eÅ ⁻³	$\nabla^2\rho$ eÅ ⁻⁵
88	O1–H1···N1	1.78	171	1 – x, y + ½, ½ – z	–7.7	0.22	0.82
	C7–H7···O1	2.73	140	1 – x, y – ½, ½ – z	0.03	0.16	
	C11–H11···O1	2.75	124	¾ – x, 1 – y, z ^o – ½	–1.6	0.04	0.17
89	O1–H1···N1	1.78	176	2 – x, 2 – y, z + ½	–9.3	0.29	0.92
	C7–H7···O1	2.72	143	2 – x, 2 – y, z – ½	0.04	0.18	
	C13–H13···F1	2.54	127	x + ½, 1 – y, z	–1.4	0.04	0.23
90	O1–H1···N1	1.87	174	1 – x, y – ½, ½ – z	–7.2	0.23	0.85
	C7–H7···O1	2.70	140	1 – x, y + ½, ½ – z	0.04	0.18	
	C11A–H11A···O1	2.68	124	¾ – x, 1 – y, z – ½	–1.3	0.02	0.18
91	C11A–H11A···F1	2.69	148	2 – x, 2 – y, -z	–1.9	0.03	0.15
	O1–H1···N2	1.92	169	x, y + 1, z	–6.4	0.29	0.91
	C20–H20···O1	2.63	156	x, y – 1, z	0.04	0.19	
	O2–H2···N1	1.86	166	x, 2 – y, z – ½	–8.9	0.24	0.89
	C7–H7···O2	2.60	156	x, 2 – y, z + ½	0.04	0.21	
	C16–H16···F2	2.61	149	–x, y + 1, ½ – z	–1.6	0.03	0.18

and c, Table 6). **95** does not have any C–H···π interaction.

5.3. Structural comparison of the compounds belonging to group 2a

The compounds **96** and **97** were found to crystallize in the non-centrosymmetric *P*2₁2₁ and *P*na₂₁ space groups respectively, while **98** and **99** were crystallized in the centrosymmetric *P*2₁/c space group (Table 7). The compounds **96**, **97** and **98** were found to have the same *R*₂²(7) dimer as was seen in the compounds belonging to group 1a and 1b (Fig. 7). The compound **98** has an additional C–H···O hydrogen bond in this dimer (Fig. 7c).

Interestingly, the compound **99** does not have the same *R*₂²(7) dimer. This has a centrosymmetric dimer through two O–H···N hydrogen bonds between the two molecules (Fig. 7d). These dimers have stabilization energies between –6.9 and –10.4 kcal/mol. In addition to these strong hydrogen bonds in **97**, **98** and **99**, various

C–H···F hydrogen bonds were identified (Fig. 8, Table 8). Once again, it was found that the compound (**99**) with fluorine at the *ortho*-position, forms a dimer (Fig. 8, Table 8) adopting the robust synthon I(A) involving C–H···F hydrogen bonds reported by us recently with the similar stabilization energy [9d]. Compounds **97** and **98** also found to have a few weak C–H···π interactions to stabilize the crystals structures (Table 9).

5.4. Structural comparison of the compounds belonging to group 2b

The compounds **100**, **101**, **102** and **103** belonging to group 2b were crystalline in nature (ESI, Fig. S4:13–16), but suitable single crystals for these compounds could not be grown by standard methods. Therefore, structures of these compounds could not be determined.

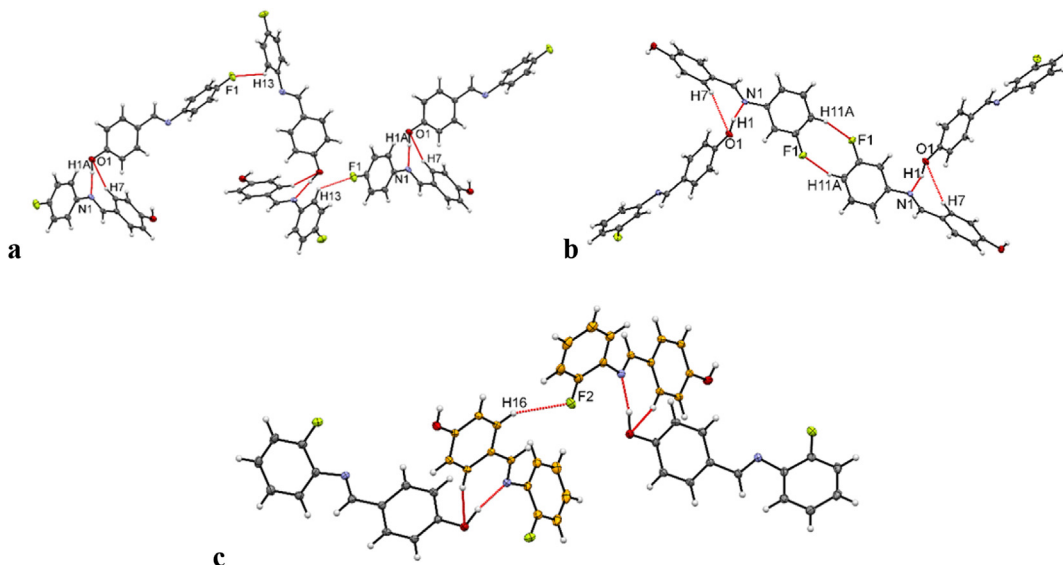


Fig. 2. (a) C–H···F hydrogen bonds in the structure **89** interlinking strong hydrogen bonded dimers (b) Centrosymmetric dimer in **90** formed through weak C–H···F hydrogen bonds, which interlinks strong hydrogen bonded dimers; (c) Weak C–H···F hydrogen bond in the structure of **91** joining the strong hydrogen bonded dimers.

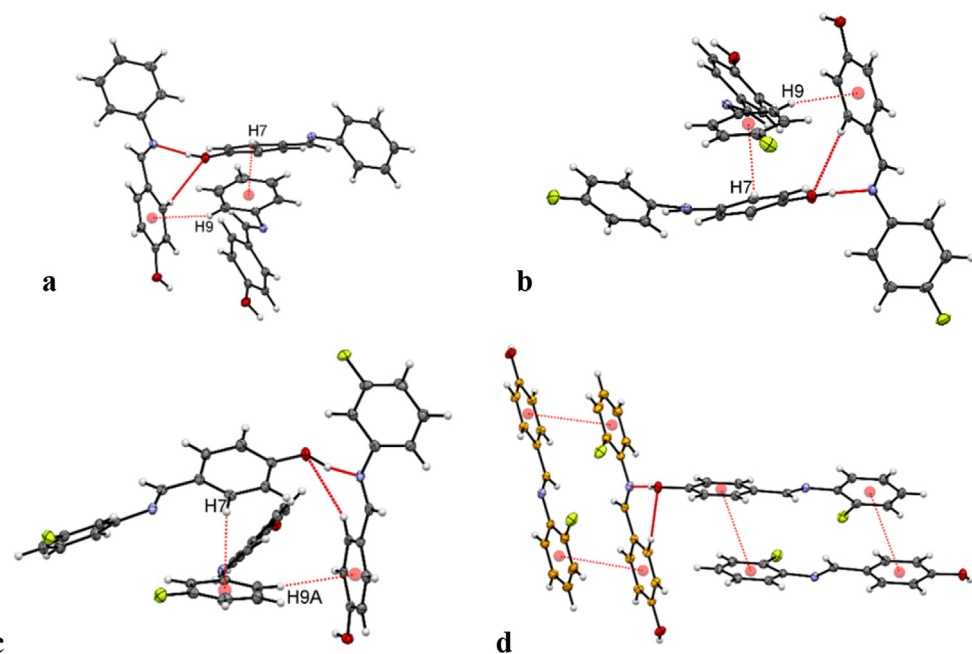


Fig. 3. C–H···π interactions in the crystal lattices of **88**, **89**, **90** and π···π interactions in **91** in figures **a**, **b**, **c** and **d** respectively.

Table 3a

Intermolecular C–H···π interactions of the compounds belonging to group 1a (**88**, **89**, **90**) compounds.

Code	C–H···π	C···π (Å)	H···π (Å)	∠C–H···π (°)	Symmetry code
88	C7–H7···Cg2	3.49	2.93	120	$\frac{1}{2} - x, \frac{1}{2} + y, z$
	C9–H9···Cg1	3.70	2.83	156	$x - \frac{1}{2}, y, \frac{1}{2} - z$
89	C7–H7···Cg2	3.35	2.83	117	$\frac{1}{2} - x, y, \frac{1}{2} + z$
	C9–H9···Cg1	3.62	2.73	157	$\frac{1}{2} + x, -y, z$
90	C7–H7···Cg2	3.46	2.89	120	$\frac{1}{2} - x, \frac{1}{2} + y, z$
	C9–H9···Cg1	3.67	2.78	157	$x - \frac{1}{2}, y, \frac{1}{2} - z$

Table 3b

Intermolecular π···π interactions of the compounds belonging to group 1a (**91**) compounds.

Code	Cg _A ···Cg _B	D (Å)	D ₁ (Å)	D ₂ (Å)	Symmetry code
91	Cg1···Cg2	3.76	3.25	3.43	$1 - x, y, \frac{1}{2} - z$
	Cg3···Cg4	3.75	3.37	3.39	$-x, y, \frac{1}{2} - z$
	Cg2···Cg2	3.82	3.53	3.53	$1 - x, -y, 1 - z$
	Cg4···Cg4	4.18	3.34	3.34	$-x, 1 - y, 1 - z$

Table 4

Unit cell parameters of the compounds belonging to group 1b (**92**, **93**, **94**, **95**) compounds.

Identification code	92	93	94	95
CCDC No.	1040702	1040703	1040704	1040705
Crystal system	Monoclinic	Monoclinic	Monoclinic	Monoclinic
Space group	$P2_1/c$	$P2_1/c$	$P2_1/c$	$P2_1/c$
$a/\text{\AA}$	6.4504(5)	9.2568(8)	6.598(2)	5.9223(6)
$b/\text{\AA}$	14.4278(11)	12.2098(10)	14.197(5)	16.9858(18)
$c/\text{\AA}$	12.7143(10)	14.5949(11)	12.582(4)	11.7847(11)
$\alpha/^\circ$	90	90	90	90
$\beta/^\circ$	121.331(5)	141.693(5)	120.439(18)	122.080(6)
$\gamma/^\circ$	90	90	90	90
Volume/ \AA^3	1010.71(14)	1022.53(16)	1016.2(6)	1004.47(18)
Z	4	4	4	4
Z'	1	1	1	1

5.5. Structural comparison of the compounds belonging to group 3a

Compounds **104** and **106** were crystallized in the non-centrosymmetric Cc and $Pca2_1$ space groups respectively, while **105** and **107** were crystallized in the centrosymmetric $P2_1/c$ space group (Table 10). All the compounds belonging to group 3a have intramolecular O–H···N hydrogen bond involving the *ortho*-hydroxyl group and the imine nitrogen (ESI (Fig. S6:13–16), Table 11). Since the –OH group is locked within the molecule in these compounds, they were packed in the lattice through various different weak C–H···O and C–H···F hydrogen bonds (Table 12, Fig. 9) and C–H···π interactions (Table 13, Fig. 9).

5.6. Structural comparison of the compounds belonging to group 3b

The compounds **108** (disordered) and **111** were crystallized in non-centrosymmetric orthorhombic space groups $Pca2_1$ and $P2_12_12_1$ respectively, while the other two compounds (**109** and **110**) were found to adopt centrosymmetric monoclinic $P2_1/c$ space group (Table 14). Once again the *ortho* hydroxyl group on the A ring was found to be locked through intramolecular O–H···N hydrogen bond (ESI (Fig. S6:17–20), Table 15). All the four compounds belonging to this group were found to have various different C–H···O, C–H···F and O–H···F (in **111**) hydrogen bonds (Fig. 10, Table 16) and weak C–H···π interaction in their crystal lattice (Fig. 10, Table 17).

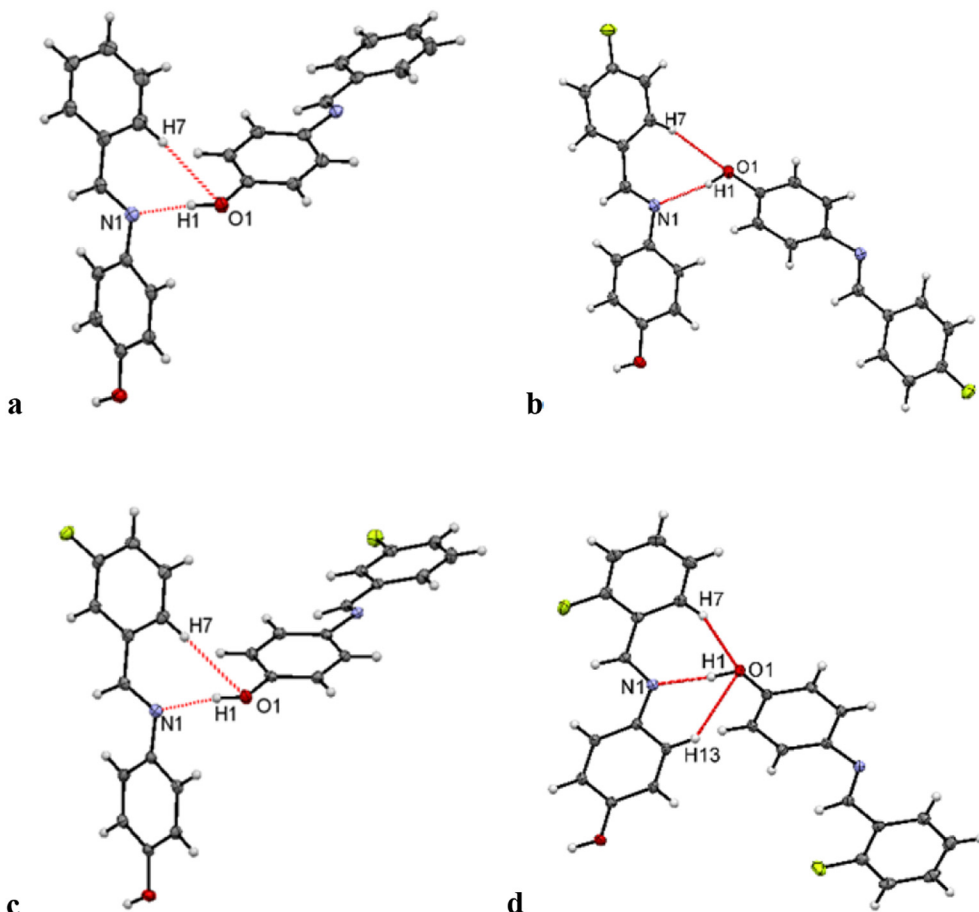
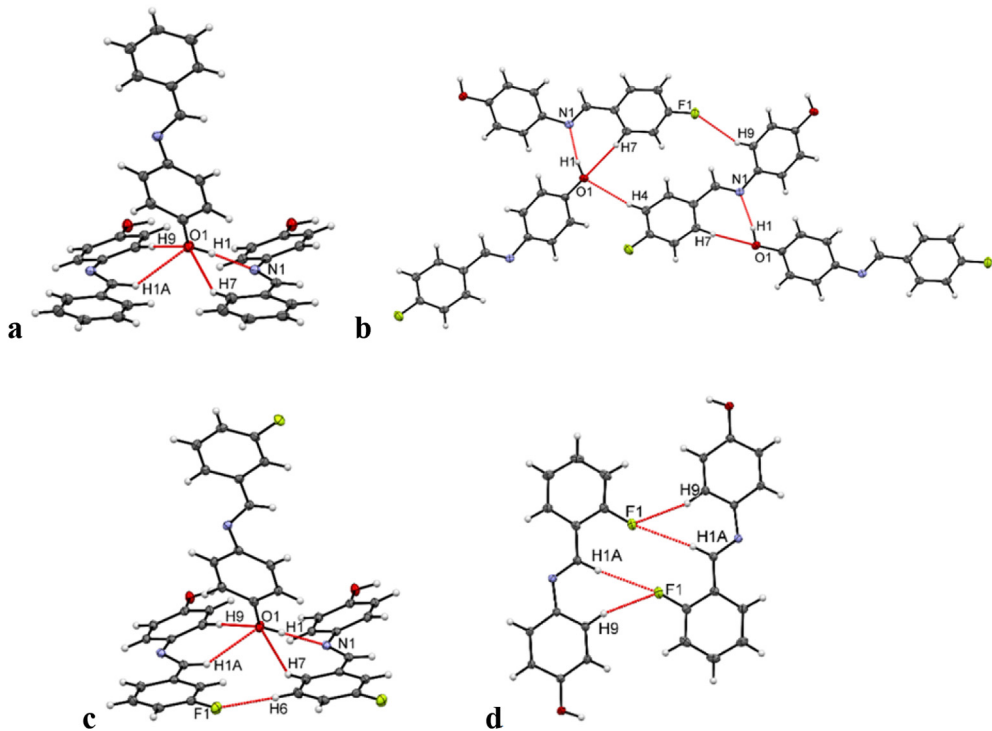


Fig. 4. Formation of strong hydrogen bonded dimers in **92**, **93**, **94** and **95** in figures **a**, **b**, **c** and **d** respectively.

Table 5Intermolecular hydrogen bonds of the compounds belonging to group 1b (**92, 93, 94, 95**) compounds.

Code	D–H···A (D = C, O; A = O, N, F)	d H···A/Å	∠D–H···A/°	Symmetry code	SE _{G09} kcal/mol	ρ eÅ ⁻³	$\nabla^2 \rho$ eÅ ⁻⁵
92	O1–H1···N1	1.81	170	x + 1, $\frac{1}{2}$ – y, z + $\frac{1}{2}$	–7.3	0.21	0.80
	C7–H7···O1	2.64	147	x – 1, $\frac{1}{2}$ – y, z – $\frac{1}{2}$	0.04	0.20	
	C1–H1A···O1	2.64	130	x, $\frac{1}{2}$ – y, z + $\frac{1}{2}$	–3.6	0.05	0.2
	C9–H9···O1	2.50	172		0.06	0.23	
93	O1–H1···N1	1.98	167	x – 1, $-\frac{1}{2}$ – y, z – $\frac{1}{2}$	–8.1	0.19	0.64
	C7–H7···O1	2.54	137	x + 1, $-\frac{1}{2}$ – y, z + $\frac{1}{2}$	0.05	0.22	
	C4–H4···O1	2.68	136	x, y + 1, z	–1.5	0.03	0.16
	C9–H9···F1	2.66	156	x – 1, $\frac{1}{2}$ – y, z – $\frac{1}{2}$	–2.3	0.03	0.16
94	O1–H1···N1	1.95	167	x, $\frac{1}{2}$ – y, z + $\frac{1}{2}$	–8.1	0.23	0.79
	C7–H7···O1	2.64	144	x, $\frac{1}{2}$ – y, z – $\frac{1}{2}$	0.04	0.21	
	C1–H1A···O1	2.65	136	x – 1, $\frac{1}{2}$ – y, z – $\frac{1}{2}$	–4.0	0.04	0.19
	C9–H9···O1	2.57	173	x – 1, $\frac{1}{2}$ – y, z – $\frac{1}{2}$	0.05	0.20	
95	C6–H6···F1	2.42	176	x + 1, y, z	–2.5	0.05	0.26
	O1–H1···N1	1.85	174	x, $\frac{3}{2}$ – y, z – $\frac{1}{2}$	–12.5	0.25	0.83
	C7–H7···O1	2.42	160	x, $\frac{3}{2}$ – y, z – $\frac{1}{2}$	0.07	0.28	
	C13–H13···O1	2.65	135	x, $\frac{3}{2}$ – y, z – $\frac{1}{2}$	0.04	0.22	
95	C1–H1A···F1	2.72	174	1 – x, 2 – y, 2 – z	–2.3	0.02	0.13
	C9–H9···F1	2.55	151	1 – x, 2 – y, 2 – z		0.04	

**Fig. 5.** C–H···O or (and) C–H···F hydrogen bonds in **a**, **b**, **c** and **d** in the compounds **92, 93, 94** and **95** respectively.

6. Discussion

From the above crystallographic data, structural descriptions and the various packing characteristics observed in the compounds

studied in this manuscript, it is evident that the hydroxyl group generally preferred to form only one type of dimer ($R_2^2(7)$), when it is at *para*- or at *meta*-positions except for the compound **99**. But the spatial dispositions of the two molecules connected by this $R_2^2(7)$

Table 6Intermolecular C–H···π interactions of the compounds belonging to group 1b (**92, 93, 94**) compounds.

Code	C–H···π	C···π (Å)	H···π (Å)	∠C–H···π (°)	Symmetry code
92	C5–H5···Cg2	3.47	2.57	158	1 – x, y – $\frac{1}{2}$, $\frac{1}{2}$ – z
93	C3–H3···Cg2	3.46	2.79	129	–x, –y, –z
	C10–H10···Cg1	3.48	2.76	133	x, y + $\frac{1}{2}$, $\frac{1}{2}$ – z
	C13–H13···Cg1	3.46	2.77	130	–x, y + $\frac{1}{2}$, $\frac{1}{2}$ – z
94	C5–H5···Cg2	3.42	2.52	158	–x, y + $\frac{1}{2}$, $\frac{1}{2}$ – z

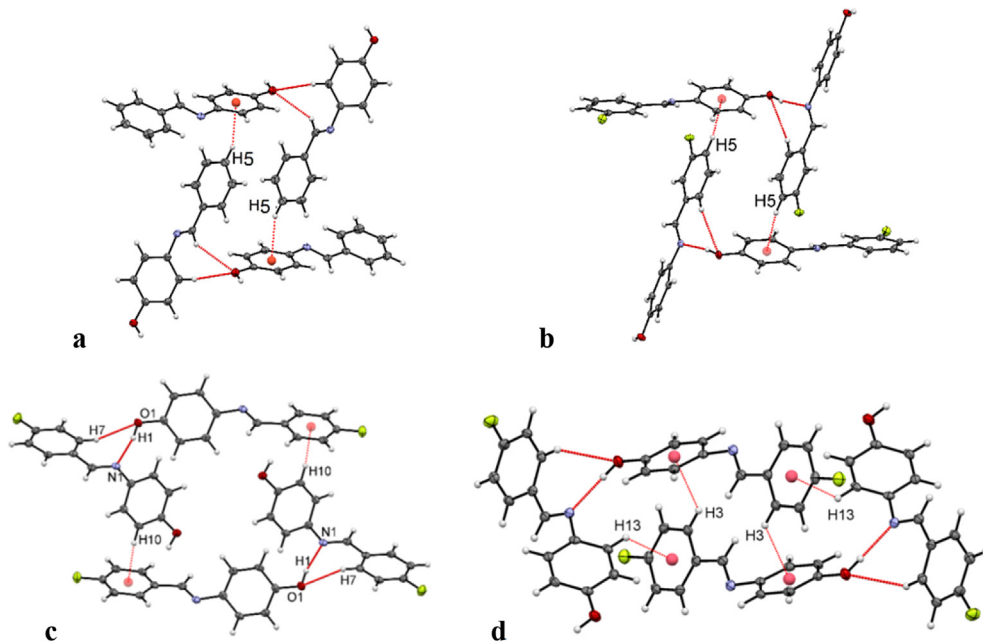


Fig. 6. C–H··· π interactions unifying the strong hydrogen bonded dimers in the crystal lattice of **92** in (a), **94** in (b) and **93** in (c) and (d).

Table 7

Unit cells parameters of the compounds belonging to group 2a (**96**, **97**, **98**, **99**) compounds.

Identification code	96	97	98	99
CCDC No.	1040706	1040707	1040708	1040709
Crystal system	Orthorhombic	Orthorhombic	Monoclinic	Monoclinic
Space group	$P_{2_1}2_1$	Pna_2_1	$P2_1/c$	$P2_1/c$
$a/\text{\AA}$	5.463(8)	16.779(2)	11.2365(6)	12.086(6)
$b/\text{\AA}$	10.613(15)	5.4254(7)	6.0355(3)	14.403(6)
$c/\text{\AA}$	17.22(3)	23.148(3)	20.7780(10)	5.855(3)
$\alpha/^\circ$	90	90	90	90
$\beta/^\circ$	90	90	133.006(3)	95.76(3)
$\gamma/^\circ$	90	90	90	90
Volume/ \AA^3	999(3)	2107.3(5)	1030.46(10)	1014.2(8)
Z	4	8	4	4
Z'	1	2	1	1

dimer were found to be different in all the compounds. Further, the angle between the two phenyl rings (Table 18) have been noted to vary significantly making the molecule planar for the cases where –OH group forms intramolecular hydrogen bond (**105–110**) and non-planar in all other cases except in **104** and **111**. These packing and conformational differences should be attributed to the fact that the fluorine atoms present in the molecules at different positions preferred to form different weak, but significantly stabilizing C–H···F hydrogen bonds. Our general observation in cases of compounds **1**, **10** and **13** [9a] suggests that the fluorine atom at the *para*-position of the phenyl ring prefers to either form one C–H···F hydrogen bond or a bifurcated C–H···F hydrogen bond as have been seen in our earlier cases reported recently [9d]. Further, the fluorine substitution at the *meta*-position have been found to form a centrosymmetric dimer in general as was also observed in our earlier reports [9c,d]. The fluorine at the *ortho*-position has been seen mostly to form dimers involving the imine hydrogen, when the same is not involved in any strong hydrogen bond. In the cases of compounds **104–111**, where the hydroxyl group is locked by intramolecular O–H···N hydrogen bonding, the calculated lattice

energies of these structures have been found to be at least 20 kJ/mol lower (102–111 kJ/mol for **104–111**, compared to 132–142 kJ/mol for **88–99**) than those packed by intermolecular O–H···N hydrogen bonds. This indicates that the stability of these crystal structures are significantly controlled by the strong hydrogen bonds while the relative packing features are controlled by the weaker C–H···F hydrogen bonds, C–H···π and π···π interactions.

From the AIM analyses, we noted that the higher values of electron density (between 0.2 and 0.3 e \AA^{-3}) and Laplacian (between 0.65 and 0.95 e \AA^{-5}) at the bond critical points indicate strong hydrogen bonds (O–H···N). The weaker hydrogen bonds, like C–H···F and C–H···O, are identified from the lower values of electron density (ρ) (between 0.02 and 0.03 e \AA^{-3}) and Laplacian ($\nabla^2\rho$) (between 0.1 and 0.3 e \AA^{-5}) at the bond critical points. The topological parameters [ρ , $\nabla^2\rho$, $V(\mathbf{r}_{\text{CP}})$, $G(\mathbf{r}_{\text{CP}})$ and $E(\mathbf{r}_{\text{CP}})$] at the (3, -1) bond critical point for C–H···F and C–H···O hydrogen bonds have been found to vary exponentially with the bond path, as was seen by us earlier [9a,c,d]. These plots along with the fitted equation and the corresponding values of R^2 are given in figure ST1 and ST2 in ESI; the values of these parameters are given in the table ST1

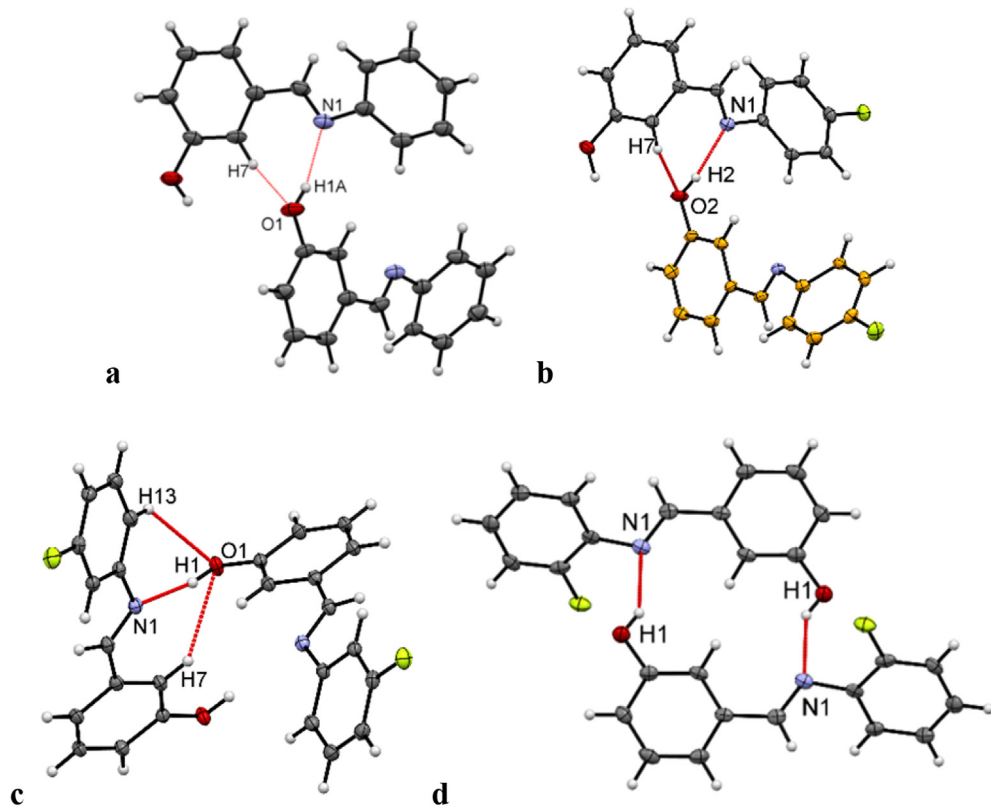


Fig. 7. (a) C–H···O and O–H···N hydrogen bonds in **96**; (b) C–H···O and O–H···N hydrogen bonded dimer between the two molecules of the asymmetric unit of **97** (c) Molecules of **98** interacting through O–H···N and C–H···O hydrogen bonds in its crystal lattice. (d) Centrosymmetric dimers formed via strong O–H···N hydrogen bonds in **99**.

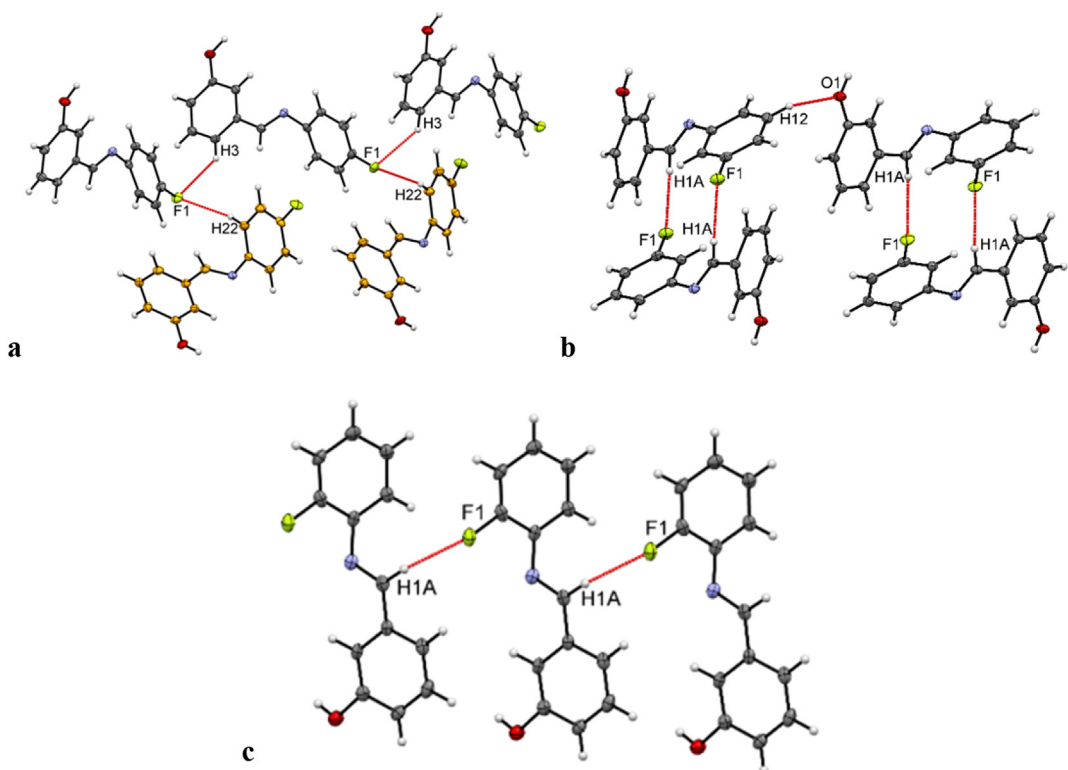


Fig. 8. (a) C–H···F intermolecular hydrogen bonds in **97** (b) C–H···O hydrogen bonds interconnecting dimers formed by C–H···F hydrogen bonds in **98**; (c) Molecular chain formation via C–H···F intermolecular hydrogen bonds involving imine hydrogen in **99**.

Table 8Intermolecular hydrogen bonds of the compounds belonging to group 2a (**96**, **97**, **98**, **99**) compounds.

Code	D–H···A (D = C, O; A = O, N, F)	d H···A/Å	∠ D–H···A/°	Symmetry code	SE _{G09} kcal/mol	ρ eÅ ⁻³	$\nabla^2\rho$ eÅ ⁻⁵
96	O1–H1···N1	1.98	158	x – ½, ¾ – y, 1 – z	–6.9	0.19	0.7
	C7–H7···O1	2.73	140	2 – x, 2 – y, z – ½	0.03	0.14	
	C12–H12···O1	2.60	123	¾ + x, ¾ – y, 1 – z	–1.2	0.05	0.21
97	O1–H1···N2	1.90	167	x, y, z	–8.2	0.21	0.76
	C20–H20···O1	2.72	147	x, y – 1, z	0.03	0.16	
	O2–H2···N1	1.78	160	x, y + 1, z	–10.1	0.28	0.86
	C7–H7···O2	2.73	147	x, y – 1, z	0.04	0.18	
	C13–H13···O2	2.54	120	x, y – 2, z	–1.2	0.06	0.25
	C3–H3···F1	2.63	136	x – ½, –y – ½, z	–2.0	0.03	0.19
	C9–H9···F2	2.47	170	½ – x, y + ½, z + ½	–2.7	0.04	0.22
98	C22–H22···F1	2.63	152	1 – x, –y, z – ½	–2.3	0.03	0.18
	O1–H1···N1	1.85	169	–x, y + ½, –z + ¾	–8.9	0.04	0.19
	C7–H7···O1	2.64	146	–x, y – ½, ¾ – z	0.04	0.2	
	C13–H13···O1	2.69	127	–x, y – ½, ¾ – z	0.04	0.19	
	C12–H12···O1	2.57	136	1 + x, ½ – y, ½ + z	–1.9	0.05	0.22
99	C1–H1A···F1	2.45	162	–x, 1 – y, 2 – z	–4.2	0.05	0.24
	O1–H1···N1 (dimer)	2.14	146	1 – x, 1 – y, 1 – z	–10.4	0.13	0.5
	C11–H11···O1	2.74	123	x + 1, y, z	–1.5	0.04	0.17
	C1–H1A···F1	2.37	159	x, y, z + 1	–5.2	0.06	0.28

Table 9Intermolecular C–H···π interactions of the compounds belonging to group 2a (**97** and **98**) compounds.

Code	C–H···π	C···π (Å)	H···π (Å)	∠ C–H···π (°)	Symmetry code
97	C4–H4···Cg2	3.61	2.70	161	½ + x, ¾ – y, z
	C17–H17···Cg4	3.74	2.84	160	½ + x, ¾ – y, z
98	C9–H9···Cg2	3.39	2.66	134	x, 1 + y, z
	C11–H11···Cg1	3.67	2.81	152	1 + x, ¾ – y, ½ + z

Table 10Unit cells parameters of the compounds belonging to group 3a (**104**, **105**, **106**, **107**) compounds.

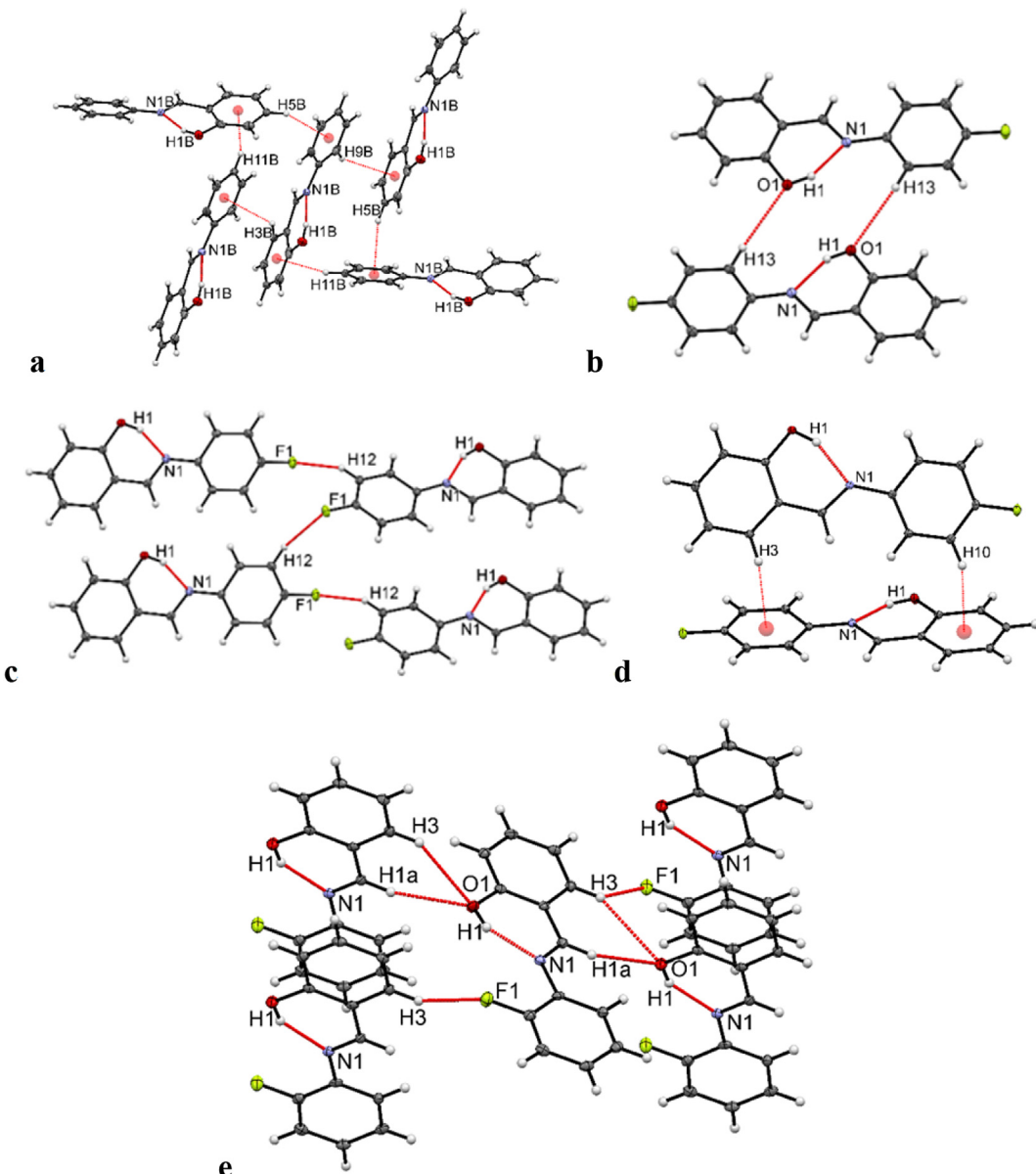
Identification code	104	105	106	107
CCDC No.	1040690	1040691	1040692	1040693
Crystal system	Monoclinic	Monoclinic	Orthorhombic	Monoclinic
Space group	Cc	P2 ₁ /c	Pca2 ₁	P2 ₁ /c
a/Å	5.8088(12)	12.6969(7)	24.8208(11)	4.6762(8)
b/Å	12.891(3)	5.7190(3)	3.8115(2)	18.667(3)
c/Å	14.025(3)	14.5222(8)	10.6318(5)	12.957(2)
$\alpha/^\circ$	90	90	90	90
$\beta/^\circ$	101.972(3)	107.1660(10)	90	116.201(11)
$\gamma/^\circ$	90	90	90	90
Volume/Å ³	1027.3(4)	1007.53(9)	1005.82(8)	1014.8(3)
Z	4	4	4	4
Z'	1	1	1	1

and ST₂ in the ESI.The lattice energies were calculated using PIXEL and various components of lattice energies are given in the Table ST₀ in the ESI. It is evident from this table that the lattice energies of thecompounds (**99**–**111**) with intramolecular O–H···N hydrogen bond were approximately 5–7 kcal/mol lower than those having intermolecular O–H···N hydrogen bond. This feature is also observed in the melting characteristic of these compounds. The compounds **88****Table 11**Geometrical parameters for intramolecular O–H···N hydrogen bonds of the compounds belonging to group 3a (**104**, **105**, **106**, **107**) compounds.

Code	O–H···N	d H···N/Å	∠ O–H···N/°	Symmetry code
104	O1–H1···N1	1.92	137	x, y, z
105	O1–H1···N1	1.78	154	x, y, z
106	O1–H1···N1	1.79	151	x, y, z
107	O1–H1···N2	1.86	146	x, y, z

Table 12Intermolecular hydrogen bonds of the compounds belonging to group 3a (**105** and **107**) compounds.

Code	C–H···A (A = O, F)	d H···A/Å	∠C–H···A/°	Symmetry code	SE _{G09} kcal/mol	ρ eÅ ⁻³	$\nabla^2\rho$ eÅ ⁻⁵
105	C13–H13···O1	2.70	160	–x, –y, –z	–3.1	0.03	0.16
	C12–H12···F1	2.62	148	1 – x, y – ½, ½ – z	–1.1	0.03	0.17
107	C1–H1A···O1	2.56	154	x + 1, ¾ – y, z + ½	–4.3	0.05	0.21
	C3–H3···O1	2.67	150	x + 1, ¾ – y, z + ½		0.04	0.17
	C3–H3···F1	2.62	126	x, ¾ – y, ½ + z	–2.0	0.03	0.19

**Fig. 9.** (a) C–H···π interactions in **104** by which molecules propagate in the lattice; (b) Formation of antiparallel dimer via C–H···O hydrogen bonds in **105**; (c) C–H···F intermolecular hydrogen bonds in **105**; (d) C–H···π interactions in **105**; (e) O–H···N (intramolecular), C–H···O and C–H···F hydrogen bond in **107**.

to **98** have higher melting point (86–186 °C) and higher melting enthalpy (19.5–44.8 kJ/mol) in general, while the same for **99** to **111** are found to be much lower. Further, the dispersion components of the lattice energy have been found to be the highest in all the compounds, especially for those compounds (**99**–**111**), which had intramolecular hydrogen bonds. This observation indicates that the weak C–H···F and C–H···O hydrogen bonds mostly offer

stabilization through dispersion forces.

All the compounds reported in this manuscript also have various weak C–H···π interactions. The contribution of these interactions cannot be ignored as they also show favourable geometrical parameters indicating a sense of directionality (d(H···π) = 2.5–2.9 Å, ∠C–H···π = 130–160°). Therefore, it can be inferred that the combined influence of a number of weak interactions (C–H···F,

Table 13

Intermolecular C–H···π interactions of the compounds belonging to group 3a (**104** and **105**) compounds.

Code	C–H···π	C···π (Å)	H···π (Å)	∠C–H···π (°)	Symmetry code
104	C3B–H3B···Cg2	3.54	2.84	131	x – ½, y – ½, z
	C5B–H5B···Cg2	3.57	2.74	146	x, –y, z – ½
	C9B–H9B···Cg1	3.53	2.83	131	x – ½, ½ + y, z
	C11B–H11B···Cg1	3.57	2.74	146	½ + x, ½ – y, ½ + z
105	C3–H3···Cg2	3.47	2.76	132	–x, ½ + y, ½ – z
	C10–H10···Cg1	3.41	2.71	131	–x, ½ + y, ½ – z

Table 14

Unit cells parameters of the compounds belonging to group 3b (**108**, **109**, **110**, **111**) compounds.

Identification code	108	109	110	111
CCDC No.	1040694	1040695	1040696	1040690
Crystal system	Orthorhombic	Monoclinic	Monoclinic	Orthorhombic
Space group	Pca ₂ ₁	P2 ₁ /c	P2 ₁ /c	P2 ₁ 2 ₁ 2 ₁
a/Å	12.1651(11)	21.6018(15)	12.330(4)	6.5279(6)
b/Å	6.0020(6)	5.9384(4)	5.8464(15)	10.9920(9)
c/Å	13.8111(13)	17.2691(12)	21.381(6)	14.3681(12)
α/°	90	90	90	90
β/°	90	113.142(4)	138.261(1)	90
γ/°	90	90	90	90
Volume/Å ³	1008.42(17)	2037.0(2)	1026.1(5)	1030.98(15)
Z	4	8	4	4
Z'	1	2	1	1

C–H···O and C–H···π) have enforced these molecules to adopt different 3D arrangements with both centrosymmetric (*Pbca*, *P2/c* and *P2₁/c*) and non-centrosymmetric (*Cc*, *Pca₂₁*, *P2₁2₁2₁* and *Pna2₁*) space groups. In addition, it is observed that even though the compounds belonging to one group are crystallized in the same space group (group **1b**) had widely different structures mostly due to differences in C–H···F, C–H···O and C–H···π interactions.

It is worth mentioning that the structures of the compounds **92** [36], **93** [37], **105** [38] and **108** [39] were reported earlier at room temperature, just as a structural report and in-depth structural analyses of these compounds were not done. Further, three polymorphs of the compound **104** [40] were reported earlier using a single crystal data recorded at 120 K. As we intended to analyse all the structures at 100 K, we made all the compounds, crystallized them and conducted the entire study at the same temperature. The polymorph of **104**, reported by us in this manuscript is different from those reported earlier.

7. Conclusions

This manuscript highlights the importance of a number of weak interactions in the presence of a strong hydrogen bond in the packing of a series of small organic molecules. Because of the strong directionality and high stabilization energy associated with the strong O–H···N hydrogen bond, these molecules generally had the *R*₂(7) dimer as the primary recognition

mechanism. The other weaker interactions have been shown to be highly influential in altering the overall packing characteristics of these molecules without significant hindrance to the strong O–H···N hydrogen bond. Although, the compounds with the –OH group at the *meta*-position of A ring were crystalline when synthesized, they did not yield suitable single crystal for structural analysis. Further, these compounds have been found to be highly unstable in solution. That is why the NMR spectra of these compounds could not be recorded. Moreover, it should be noted that the presence of F at the *meta*-position of A or B ring does not alter the packing of molecules in the crystal lattice of the compounds belonging to group 1a and 1b (–OH group at *para*-position; compounds **88–95**). Therefore, the compounds **88** and **90**; **92** and **94**; are found to be isostructural with similar unit cell parameters and the packing characteristics. Intramolecular O–H···N hydrogen bond in the compounds **104–111** have been found to be responsible for locking the compounds in a near planar conformation, thereby allowing the weaker hydrogen bonds to completely control the structural features. As a result, a wide variation in the unit cell parameters and space groups have been seen in these compounds. Based on the results described above, it may be concluded that the supramolecular recognition patterns of various organic molecules can be altered by a number of much weaker interactions even in the presence of strong hydrogen bonds as shown here.

Table 15

Intramolecular O–H···N hydrogen bond of the compounds belonging to group 3b compounds.

Code	O–H···N	d H···N/Å	∠O–H···N/°	Symmetry code
108	O1–H1···N1	2.10	118	x, y, z
	O1–H1···N1	2.01	114	x, y, z
	O2–H2···N2	1.88	127	x, y, z
110	O1–H1···N1	2.01	117	x, y, z
	O1–H1···N1	2.14	120	x, y, z

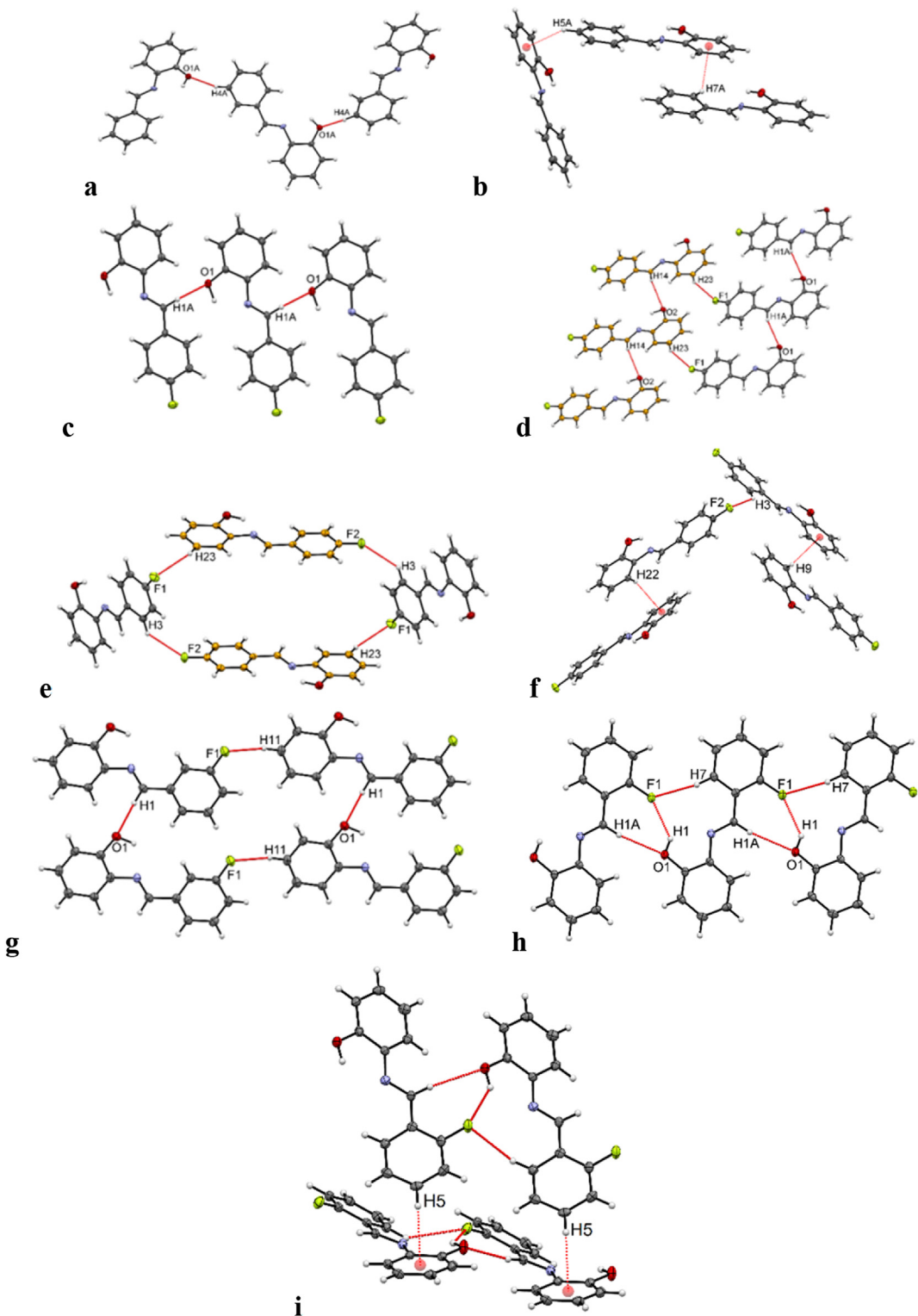


Fig. 10. (a) C–H···O intermolecular hydrogen in **108**; (b) C–H···π interactions in the crystal lattice of **108**; (c) C–H···O intermolecular hydrogen bonds in **109**; (d) C–H···O and C–H···F intermolecular hydrogen bonds in **109**; (e) Tetrameric unit formation by C–H···F hydrogen bonds in **109**; (f) C–H···π interactions in the crystal lattice of **109**; (g) Formation of molecular layers through C–H···O and C–H···F hydrogen bonds in **110**; (h) Formation of molecular chain via C–H···O, C–H···F and O–H···F hydrogen bonds in the structure of compound **111**; (i) C–H···π interactions interconnecting the above formed chains in the lattice of **111**.

Table 16

Intermolecular hydrogen bonds of the compounds belonging to group 3b (**108**, **109**, **110**, **111**) compounds.

Code	D–H···A (D = C, O; A = O, F)	d H···A/Å	∠D–H···A/°	Symmetry code	SE _{G09} kcal/mol	ρ eÅ ⁻³	$\nabla^2\rho$ eÅ ⁻⁵
108	C4A–H4A···O1	2.54	141	$\frac{1}{2} - x, y - 1, z - \frac{1}{2}$	-1.4	0.06	0.24
	C1–H1A···O1	2.57	124	$x, y - 1, z$	-4.2	0.05	0.23
	C14–H14···O2	2.61	126	$x, y - 1, z$	-4.3	0.05	0.2
	C3–H3···F2	2.69	129	$x, \frac{1}{2} - y, z - \frac{1}{2}$	-1.0	0.03	0.15
	C16–H16···F1	2.67	131	$x, y - 1, z$	-2.7	0.03	0.16
	C23–H23···F1	2.65	145	$1 - x, y - \frac{1}{2}, \frac{1}{2} - z$	-2.1	0.03	0.17
110	C1–H1A···O1	2.70	125	$x, y - 1, z$	-4.5	0.04	0.18
	C11–H11···F1	2.65	145	$x + 1, y, z$	-0.7	0.03	0.17
111	C1–H1A···O1	2.53	169	$x - 1, y, z$	-3.7	0.05	0.21
	C7–H7···F1	2.66	143	$x + 1, y, z$	0.03	0.16	
	O1–H1···F1	2.26	134	$x + 1, y, z$	0.06	0.34	

Table 17

Intermolecular C–H···π interactions of the compounds belonging to group 3b (**108**, **109**, **110**, **111**) compounds.

Code	C–H···π	C···π (Å)	H···π (Å)	∠C–H···π (°)	Symmetry code
108	C5A–H5A···Cg2	3.57	2.84	135	$\frac{1}{2} - x, y, z - \frac{1}{2}$
	C7A–H7A···Cg2	3.43	2.79	125	$\frac{1}{2} + x, 2 - y, z$
	C9A–H9A···Cg1	3.68	2.94	136	$x - \frac{1}{2}, 1 - y, z$
109	C9–H9···Cg2	3.50	2.78	134	$-x, \frac{1}{2} + y, \frac{1}{2} - z$
	C22–H22···Cg4	3.48	2.77	132	$1 - x, y - \frac{1}{2}, \frac{1}{2} - z$
110	C4–H4···Cg1	3.57	2.88	130	$1 - x, y - \frac{1}{2}, \frac{1}{2} - z$
	C9–H9···Cg2	3.44	2.72	133	$-x, y - \frac{1}{2}, \frac{1}{2} - z$
111	C5–H5···Cg2	3.36	2.59	138	$2 - x, y - \frac{1}{2}, \frac{1}{2} - z$

Table 18

List of the angle between the two phenyl rings in **88**–**111**.

Compound no	∠Ar···Ar/°	Compound no	∠Ar···Ar/°
88	54.5	100	—
89	51.0	101	—
90	52.7	102	—
91	40.1, 37.9	103	—
92	18.9	104	50.0
93	54.5	105	2.0
94	14.9	106	7.1
95	6.5	107	4.9
96	21.4	108	0.5
97	39.8, 33.3	109	0.4, 0.8
98	44.6	110	1.0
99	53.5	111	30.0

Acknowledgements

Authors thank IISER Mohali for financial and all infrastructural supports including X-ray diffraction, NMR, DSC and all other research facilities. SS and AS thank DST INSPIRE for fellowship and GK thanks CSIR for SRF. The experimental work reported in this manuscript are parts of summer projects conducted in 2013 and 2014.

Appendix A. Supplementary data

Supplementary data related to this article can be found at <http://dx.doi.org/10.1016/j.molstruc.2015.10.105>.

References

- [1] (a) G.R. Desiraju, Crystal Engineering: the Design of Organic Solids, Elsevier, Amsterdam, 1989;
 (b) G.R. Desiraju, *Angew. Chem. Int. Ed. Engl.* **46** (2007) 8342–8356;
 (c) G.R. Desiraju, *J. Chem. Sci.* **122** (2010) 667–675;
 (d) T.N. Guru Row, *Coord. Chem. Rev.* **183** (1999) 81–100 (and references therein);
 (e) G.M.J. Schmidt, *Pure Appl. Chem.* **27** (1971) 647;
 (f) C.B. Aakeröy, K.R. Seddon, *Chem. Soc. Rev.* **22** (1993) 397–407;
- [2] (a) B. Moulton, M.J. Zaworotko, *Chem. Rev.* **101** (2001) 1629–1658;
 (b) R. Bishop, Crystal engineering, in: Kirk-Othmer Encyclopedia of Chemical Technology, 2014, pp. 1–31.
- [3] (a) A. Nangia, Molecular conformation and crystal lattice energy factors in conformational polymorphs, in: C.A. Jan Boeyens, J.F. Ogilvie (Eds.), Models, Mysteries and Magic of Molecules, Springer, Netherlands, 2008, pp. 63–86;
 (b) S. Roy, R. Banerjee, A. Nangia, G. Kruger, *J. Chem. Eur. J.* **12** (2006) 3777–3788.
- [4] (a) H. Nowell, S.L. Price, *Acta Cryst. B61* (2005) 558–568;
 (b) R. Taylor, O. Kennar, *Acc. Chem. Res.* **17** (1984) 320–326;
 (c) G.A. Jeffrey, *An Introduction to Hydrogen Bonding*, Oxford University Press, USA, 1997;
 (d) G.R. Desiraju, T. Steiner, *The Weak Hydrogen Bond in Structural Chemistry and Biology*, Oxford University Press, Oxford, 1999;
 (e) C.B. Aakeröy, T.A. Evans, K.R. Seddon, I. Pálánkó, *New J. Chem.* **23** (1999) 145–152;
 (f) S.C. Zimmerman, P.S. Corbin, *Struct. Bond.* **96** (2000) 63–94;
 (g) G.A. Jeffrey, *J. Crystallogr. Rev.* **9** (2003) 135–176;
 (h) T. Steiner, *J. Crystallogr. Rev.* **9** (2003) 177–228;
 (i) V.N. Yadav, C.H. Görbitz, *CrystEngComm* **15** (2013) 7321–7326;
 (j) J.D. Virdo, L. Crandall, J.D. Dang, M.V. Fulford, A.J. Lough, W.S. Durfee, T.P. Bender, *CrystEngComm* **15** (2013) 8578–8586.
- [5] (a) Z. Han, Y. Zhao, J. Peng, A. Tian, Q. Liu, J. Ma, E. Wang, N. Hu, *CrystEngComm* **7** (2005) 380–387;
 (b) L.C. Roper, C. Prasang, V.N. Kozhevnikov, A.C. Whitwood, P.B. Karadakov, D.W. Bruce, *Cryst. Growth Des.* **10** (2010) 3710–3720;
 (d) M. Baldrihi, D. Bartesaghi, G. Cavallo, M.R. Chierotti, R. Gobetto, P. Metrangolo, T. Pilati, G. Resnati, G. Terraneo, *CrystEngComm* **16** (2014) 5897–5904.
- [6] (a) M. Nishio, M. Hirota, *Tetrahedron* **45** (1989) 7201–7245;
 (b) M. Nishio, Y. Umezawa, M. Hirota, Y. Takeuchi, *Tetrahedron* **51** (1995) 8665–8701;
 (c) J.F. Malone, C.M. Murray, M.H. Charlton, R. Docherty, A.J. Lavery, *J. Chem. Soc. Faraday Trans.* **93** (1997) 3429–3436.
- [7] (a) C. Claessens, J. Stoddart, *J. Phys. Org. Chem.* **10** (1997) 254–272;
 (b) F. Yang, P.E. Fanwick, C.P. Kubik, *Inorg. Chem.* **41** (2002) 4805–4809;
 (c) V. Percec, M. Glodde, T. Bera, Y. Miura, I. Shiyanovskaya, K. Singer, V. Balagurusamy, P. Heiney, I. Schnell, A. Rapp, *Nature* **417** (2002) 384–387.
- [8] (a) D. Chopra, T.N. Guru Row, *CrystEngComm* **10** (2008) 54–67;
 (b) S.K. Nayak, K.N. Venugopala, D. Chopra Vasu, T.N. Guru Row, *CrystEngComm* **12** (2010) 1205–1216;
 (c) S.K. Nayak, M.K. Reddy, T.N. Guru Row, D. Chopra, *Cryst. Growth Des.* **11** (2011) 1578–1596;
 (d) P. Panini, D. Chopra, *CrystEngComm* **14** (2012) 1972–1989.
- [9] (a) G. Kaur, P. Panini, D. Chopra, A.R. Choudhury, *Cryst. Growth Des.* **12** (2012) 5096–5110;
 (b) M. Karanam, A.R. Choudhury, *Cryst. Growth Des.* **13** (2013) 4803–4814;

- (c) G. Kaur, A.R. Choudhury, *Cryst. Growth Des.* 14 (2014) 1600–1616;
 (d) G. Kaur, A.R. Choudhury, *CrystEngComm* 17 (2015) 2949–2963;
 (e) S. Dev, S. Maheshwari, A.R. Choudhury, *RSC Adv.* 5 (2015) 26932–26940.
- [10] J.D. Dunitz, R. Taylor, *Chem. Eur. J.* 3 (1997) 89–98.
- [11] (a) N. Ramasubbu, R. Parthasarathy, P.M.-. Rust, *J. Am. Chem. Soc.* 108 (1986) 4308–4314;
 (b) L. Shimoni, J.P. Glusker, *Struct. Chem.* 5 (1994) 383–397;
 (c) J.A.K. Howard, V.J. Hoy, D. O'Hagan, G.T. Smith, *Tetrahedron* 52 (1996) 12613–12622.
- [12] V.R. Thalladi, H.C. Weiss, D. Bläser, R. Boese, A. Nangia, G.R. Desiraju, *J. Am. Chem. Soc.* 120 (1998) 8702–8710.
- [13] (a) A.R. Choudhury, K. Islam, M.T. Kirchner, G. Mehta, T.N. Guru Row, *J. Am. Chem. Soc.* 126 (2004) 12274–12275;
 (b) A.R. Choudhury, N. Winterton, A. Steiner, A.I. Cooper, K.A. Johnson, *J. Am. Chem. Soc.* 127 (2005) 16792–16793;
 (c) A.R. Choudhury, D.S. Yufit, J.A.K. Howard, Z. Krist. 229 (2014) 625–634.
- [14] (a) A.R. Choudhury, U.K. Urs, T.N. Guru Row, K. Nagarajan, *J. Mol. Struct.* 605 (2002) 71–77;
 (b) A.R. Choudhury, K. Nagarajan, T.N. Guru Row, *Cryst. Eng.* 6 (2003) 43–55;
 (c) A.R. Choudhury, T.N. Guru Row, *Cryst. Growth Des.* 4 (2004) 47–52;
 (d) A.R. Choudhury, K. Nagarajan, T.N. Guru Row, *Acta Crystallogr. Sect. C. Cryst. Struct. Commun.* 60 (2004) 0644–0647;
 (e) A.R. Choudhury, T.N. Guru Row, *CrystEngComm* 8 (2006) 265–274;
 (f) R. Mariaca, N.-R. Behrnd, P. Eggl, H. Stoeckli-Evans, J. Hulliger, *CrystEngComm* 8 (2006) 222–232.
- [15] R. Berger, G. Resnati, P. Metrangolo, E. Weber, J. Hulliger, *Chem. Soc. Rev.* 40 (2011) 3496–3508.
- [16] D. Chopra, T.N. Guru Row, *CrystEngComm* 13 (2011) 2175–2186.
- [17] D. Chopra, *Cryst. Growth Des.* 12 (2012) 541–546.
- [18] V.R. Hathwar, D. Chopra, P. Panini, T.N. Guru Row, *Cryst. Growth Des.* 14 (2014) 5366–5369.
- [19] S.L. James, C.J. Adams, C. Bolm, D. Braga, P. Collier, T. Friscic, F. Grepioni, K.D.M. Harris, G. Hyett, W. Jones, A. Krebs, J. Mack, L. Maini, A.G. Orpen, I.P. Parkin, W.C. Shearouse, J.W. Steedk, D.C. Waddelli, *Chem. Soc. Rev.* 41 (2012) 413–447.
- [20] C.F. Macrae, I.J. Bruno, J.A. Chisholm, P.R. Edgington, P. McCabe, E. Pidcock, L. Rodriguez-Monge, R. Taylor, J. van de Streek, P.A. Wood, *J. Appl. Crystallogr.* 41 (2008) 466–470.
- [22] APEX2, SADABS and SAINT, Bruker AXS Inc., Madison, Wisconsin, USA, 2008.
- [23] CrystalClear 2.0, Rigaku Corporation, Tokyo, Japan.
- [24] G.M. Sheldrick, *Acta Crystallogr. A* 64 (2008) 112–122.
- [25] O.V. Dolomanov, L.J. Bourhis, R.J. Gildea, J.A.K. Howard, H. Puschmann, *J. Appl. Crystallogr.* 42 (2009) 339–341.
- [26] M. Nardelli, *J. Appl. Crystallogr.* 28 (1995) 569.
- [27] A.L. Spek, *Acta Crystallogr. D65* (2009) 148–155.
- [28] C. Möller, M.S. Plessset, *Phys. Rev.* 46 (1934) 618–622.
- [29] M.J. Frisch, G.W. Trucks, H.B. Schlegel, G.E. Scuseria, M.A. Robb, J.R. Cheeseman, G. Scalmani, V. Barone, B. Mennucci, G.A. Petersson, H. Nakatsuji, M. Caricato, X. Li, H.P. Hratchian, A.F. Izmaylov, J. Bloino, G. Zheng, J.L. Sonnenberg, M. Hada, M. Ehara, K. Toyota, R. Fukuda, J. Hasegawa, M. Ishida, T. Nakajima, Y. Honda, O. Kitao, H. Nakai, T. Vreven, J.A. Montgomery Jr., J.E. Peralta, F. Ogliaro, M. Bearpark, J.J. Heyd, E. Brothers, K.N. Kudin, V.N. Staroverov, R. Kobayashi, J. Normand, K. Raghavachari, A. Rendell, J.C. Burant, S.S. Iyengar, J. Tomasi, M. Cossi, N. Rega, J.M. Millam, M. Klene, J.E. Knox, J.B. Cross, V. Bakken, C. Adamo, J. Jaramillo, R. Gomperts, R.E. Stratmann, O. Yazyev, A.J. Austin, R. Cammi, C. Pomelli, J.W. Ochterski, R.L. Martin, K. Morokuma, V.G. Zakrzewski, G.A. Voth, P. Salvador, J.J. Dannenberg, S. Dapprich, A.D. Daniels, Ö. Farkas, J.B. Foresman, J.V. Ortiz, J. Cioslowski, D.J. Fox, Gaussian 09, Revision A.1, Gaussian, Inc., Wallingford, CT, 2009.
- [30] S.F. Boys, F. Bernardi, *Mol. Phys.* 19 (1970) 553–566.
- [31] R. Dennington, T. Keith, J. Millam, GaussView, Version 5, Semichem Inc., Shawnee Mission KS, 2009.
- [32] A. Gavezzotti, *New J. Chem.* 35 (2011) 1360–1368.
- [33] (a) R.F. Bader, *Atoms in Molecules. A Quantum Theory*, Clarendon Press, Oxford, UK, 1990;
 (b) F.B. König, J. Schönbohm, D. Bayles, *J. Comput. Chem.* 22 (2001) 545–559;
 (c) F.B. König, J. Schönbohm, D. Bayles, *J. Comput. Chem.* 23 (2002) 1489–1494.
- [34] SigmaPlot, Version 12.2, Systat Software, Inc., San Jose, CA, 2011.
- [35] (a) M.C. Etter, *J. Phys. Chem.* 95 (1991) 4601–4610;
 (b) J. Bernstein, R.E. Davis, L. Shimoni, N.-L. Chang, *Angew. Chem. Int. Ed. Engl.* 34 (1995) 1555–1573.
- [36] R.L. De, M. Mandal, L. Roy, J. Mukherjee, *Indian J. Chem. Sect. A* 47A (2008) 207–213.
- [37] L.-X. Sun, Y.-D. Yu, G.-Y. Wei, *Acta Crystallogr. Sect. E Struct. Rep. Online* E67 (2011) o1578.
- [38] J. Burgess, J. Fawcett, D.R. Russell, S.R. Gilani, V. Palma, *Acta Crystallogr. Sect. C. Cryst. Struct. Commun.* C55 (1999) 1707–1710.
- [39] H.-F. Guo, Y. Pan, D.-Y. Ma, K. Lu, L. Qin, *Transit. Met. Chem.* 37 (2012) 661–669.
- [40] (a) F. Arod, M. Gardon, P. Pattison, G. Chapuis, *Acta Crystallogr. Sect. C. Cryst. Struct. Commun.* C61 (2005) o317–o320;
 (b) F. Arod, P. Pattison, K.J. Schenk, G. Chapuis, *Cryst. Growth Des.* 7 (2007) 1679–1685.